Comput. Methods Appl. Mech. Engrg. 198 (2009) 947–957

Contents lists available at ScienceDirect

Comput. Methods Appl. Mech. Engrg.

journal homepage: www.elsevier.com/locate/cma

A parallel domain decomposition method for coupling of surface and groundwater flows

Bin Jiang *

Department of Mathematics and Statistics, Portland State University, Portland, OR 97201, USA

ARTICLE INFO

Article history:
Received 16 May 2007
Received in revised form 30 September 2008
Accepted 3 November 2008
Available online 12 November 2008

Keywords:
Coupling of surface and groundwater flows
Domain decomposition
Mixed finite element method

ABSTRACT

In this paper, we construct a robust parallel method based on a recently developed non-overlapping domain decomposition methodology to accurately model natural coupling of surface and groundwater flows. Stokes and Darcy equations are formulated and solved within the surface and subsurface regions, respectively. A new type of Robin–Robin boundary condition is proposed on the common boundary for the coupling of those systems. The formulation provides great flexibility for multi-physics coupling and is suitable for efficient parallel implementation. Meanwhile, it is stable with inherent system parameter variation. A numerical example is provided to verify the theory.

1. Introduction

In this paper, we consider coupling between surface and groundwater flows, one of the most important environmental issues in the world. It includes how the pollution from the lakes and rivers makes its way into the water supply. This coupling is also important in technological applications involving filtration. The mathematical and numerical analysis of the model for the coupled problem has been well established in recent years [3,8,13,15,17]. The model consists of the Navier–Stokes equation for the fluid region coupled across an interface with the Darcy equation for the filtration velocity in the porous medium. However, most of the numerical algorithms are sequential methods and cannot fully utilize the parallel computing resources to improve their numerical performance. The objective of this paper is to construct a new iterative parallel algorithm based on a recently developed non-overlapping domain decomposition (DD) methodology to model the coupling problem accurately and efficiently. Meanwhile, the performance of the new algorithm will not be affected by parameter variations.

First, let us quickly review the related research in this field. In [13], Layton et al. consider a formulation based on the Beavers–Joseph–Saffman interface conditions, prove the existence and uniqueness of a weak solution, and analyze a continuous finite element scheme coupled with a mixed finite element method. In [17], Riviere and Yotov employ the mixed finite element method for the Darcy region and the discontinuous Galerkin method for the Stokes region. In [15], Mardal et al. apply finite element method to solve a singularly perturbed Stokes problem with Darcy flow as a limiting case. Other interesting computational studies of the coupled problem can be found at Gartling et al. [8], Salinger et al. [18], and Galvis and Sarkis [7]. All these approaches use various *ad hoc* interface decoupling strategies. However, no parallel algorithms are constructed therein.

Most recently, Discacciati et al. [3–6] solved the coupled problem where the Darcy equation is replaced by a scalar elliptic problem for the sole piezometric head ϕ. Several sequential DD methods of either Dirichlet–Neumann or Robin–Robin types based on the choice of the fluid normal velocity across the interface were proposed and analyzed such that the number of required iterations for convergence is independent of the mesh parameter h, for suitable conforming finite element approximations of the coupled problem. In order to utilize parallel computing power to solve the problem, a parallel DD method was proposed in [6]. The numerical results showed that although the number of iterations is indeed independent of the mesh size h, it can still become very large when the viscosity ν tends to small values. An Aitken acceleration technique was then applied to this DD method so that better convergence results were observed for the improved method when ν is small.

In this paper, we will propose a new parallel algorithm based on the non-overlapping DD method with Robin conditions on the interface to solve the coupled Stokes and Darcy flows. Convergence of this new algorithm needs to be set up from both analytic and discrete levels. The number of iterations for convergence should be independent of the fluid viscosity ν and the porous medium conductivity tensor K without using any Aitken acceleration technique, which will complicate the algorithm and also prevent

---

* Tel.: +1 503 725 8294; fax: +1 503 725 3661.
E-mail address: bjiang@pdx.edu
URL: http://www.mth.pdx.edu/~bjiang

0045-7825/$ - see front matter © 2008 Elsevier B.V. All rights reserved.
doi:10.1016/j.cma.2008.11.001

us from setting up an explicit formula for the error reduction factor.

This paper is organized as follows. In Section 2, we set up the formulation of coupling of surface and groundwater flows. In Section 3, a new parallel non-overlapping DD algorithm is then introduced at the analytic level. Error estimate of the iterative solutions towards the original solution shows that the convergence rate is independent of the parameter variation. In Section 4, finite element discretization of the analytic problem is set up and the discretized DD method achieves a similar error estimate. In Section 5, the DD algorithm is applied to solve a model problem of coupled Stokes and Darcy flows. The numerical result confirms the theory. Comparison with the parallel DD algorithm from [6] shows that our new algorithm has a better numerical performance. In Section 6, conclusion of the paper and some future research highlights are given.

2. Problem formulation

Let us set up the mathematical model at first. Let Ω be a bounded domain in R^d, $d=2,3$ decomposed in two non-intersecting sub-domains Ω_f filled by a fluid and Ω_p formed by a porous medium which are separated by an interface Γ, shown in Fig. 1. The other parts of the boundaries of Ω_f and Ω_p are denoted by $\Gamma_f=\partial\Omega_f\setminus\Gamma$ and $\Gamma_p=\partial\Omega_p\setminus\Gamma$, respectively. Let u_f and p_f denote the fluid velocity and pressure in Ω_f and $\phi=z+\frac{p_p}{\rho_p g}$ denote the piezometric head with z the elevation height, p_p the pressure and $\rho_p>0$ density of the fluid in Ω_p. The flow in the domain Ω_f satisfies the Stokes equation and the flow in the domain Ω_p satisfies the Darcy equation as follows:

$$\begin{cases} -\nabla\cdot T(u_f,p_f) & =f \quad \text{in} \quad \Omega_f,\\ \nabla\cdot u_f & =0 \quad \text{in} \quad \Omega_f,\\ u_f & =0 \quad \text{on} \quad \Gamma_f. \end{cases} \tag{1}$$

$$\begin{cases} -\nabla\cdot(k_p\nabla\phi) & = \quad 0 \quad \text{in} \quad \Omega_p,\\ \phi & = \quad 0 \quad \text{on} \quad \Gamma_p, \end{cases} \tag{2}$$

where $T(u_f,p_f)=-p_fI+2\nu D(u_f)$ is the stress tensor with $D(u_f)=\frac{1}{2}(\nabla u_f+\nabla u_f^T)$ the strain tensor. ν is the viscosity of the fluid, k_p is the hydraulic conductivity of the homogeneous porous media whose conductivity tensor is $K=diag(k_p,\ldots,k_p)$.

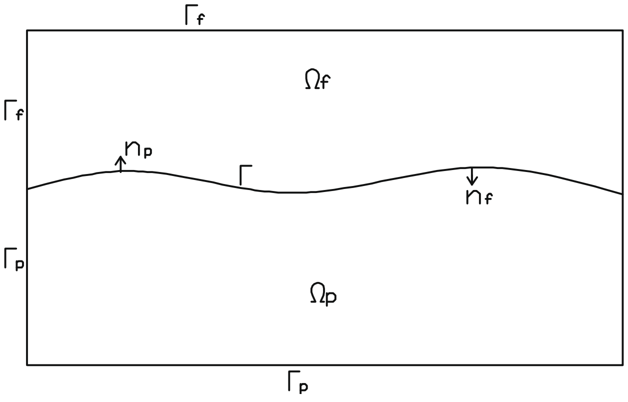

Fig. 1. Coupled fluid and porous media regions.

These equations are coupled with proper interface conditions. To ensure the continuity of the normal velocity and the normal component of the normal stress across Γ, we have

$$\begin{cases} -(k_p\nabla\phi)\cdot n=u_f\cdot n\\ g\phi=-n\cdot(T(u_f,p_f)\cdot n) \end{cases} \quad \text{on } \Gamma, \tag{3}$$

where $n=n_f$ denotes the default normal direction to Γ and then $n_p=-n$. Meanwhile, Beavers–Joseph–Saffman friction condition [10] implies

$$\nu u_f\cdot\tau_j=-\epsilon\tau_j\cdot(T(u_f,p_f)\cdot n_f), \quad j=1,\ldots,d-1, \quad \text{on } \Gamma,$$

where ϵ represents the characteristic length of the porous medium pores and τ_j, $j=1,\ldots,d-1$ are linearly independent unit tangential vectors to Γ. Since ϵ is usually much smaller than other quantities, let us simplify the above condition as follows:

$$u_f\cdot\tau_j=0, \quad j=1,\ldots,d-1, \quad \text{on } \Gamma. \tag{4}$$

The coupled system (1)–(4) has the following weak formulation which yields a unique solution based on Brezzi's theory [1].

Find $(u_f,p_f)\in H_f\times Q_f$, $\phi\in H_p$ such that

$$\begin{cases} a_f(u_f,v) & + & b_f(v,p_f)+ga_p(\phi,\psi)+\int_\Gamma g\phi(v\cdot n)-\int_\Gamma g\psi(u_f\cdot n)\\ & = & \int_{\Omega_f} f\cdot v \quad \forall v\in H_f, \quad \psi\in H_p,\\ b_f(u_f,q) & = & 0 \quad \forall q\in Q_f, \end{cases} \tag{5}$$

where

$$\begin{aligned} &H_f=\{v\in(H^1(\Omega_f))^d : v|_{\Gamma_f}=0, v\cdot\tau_j|_\Gamma=0, 1\leqslant j\leqslant d-1\},\\ &Q_f=L^2(\Omega_f),\\ &H_p=\{\psi\in H^1(\Omega_p):\psi=0 \text{ on } \Gamma_p\},\\ &a_f(u,v)=2\nu\int_{\Omega_f}D(u):D(v), \quad b_f(v,q)=-\int_{\Omega_f}q\nabla\cdot v,\\ &a_p(\phi,\psi)=\int_{\Omega_p}k_p\nabla\phi\cdot\nabla\psi. \end{aligned}$$

In this paper, we will construct a robust parallel DD method whose number of iterations is insensitive to the parameters ν and k_p. In fact, such a non-overlapping DD method was successfully applied to solve free seepage fluid flow in porous media in [11,12], where convergence of the iterative solutions towards the original solution was provided at both analytic and discrete levels. We are then motivated to apply this DD method in solving coupled groundwater and surface flows, which is much more complicated than free seepage problem.

3. Parallel domain decomposition algorithm

3.1. Old parallel DD algorithm

Before introducing our new parallel algorithm, let us review a Robin–Robin DD method constructed by Discacciati et al. [6], which is the only reported parallel DD algorithm in solving coupled system of Stokes and Darcy flows.

Algorithm 0. Let $\mu^1=0$ be an assigned trace function on Γ, and let γ_1, γ_2 be two positive parameters; then, repeat the following three steps for $k=1,2,\ldots$ until convergence.

Step 1. Solve $(u_f^k,p_f^k)\in H_f\times Q_f$ and $\phi^k\in H_p$ such that

$$\begin{cases} a_f(u_f^k,v)+b_f(v,p_f^k) & -\gamma_1\int_\Gamma(u_f^k\cdot n)(v\cdot n)\\ & =\int_\Gamma\mu^k(v\cdot n)+\int_{\Omega_f}f\cdot v \quad \forall v\in H_f,\\ b_f(u_f^k,q)=0 & \forall q\in Q_f, \end{cases}$$

and

$$a_p(\phi^k,\psi)+\frac{1}{\gamma_1}\int_\Gamma g\phi^k\psi=-\frac{1}{\gamma_1}\int_\Gamma\mu^k\psi \quad \forall\psi\in H_p.$$

Step 2. Compute $\hat{\sigma}^k=u_f^k\cdot n+k_p\nabla\phi^k\cdot n=u_f^k\cdot n+\frac{1}{\gamma_1}(g\phi^k+\mu^k)$ on Γ. Then, solve $(\hat{u}_f^k,\hat{p}_f^k)\in H_f\times Q_f$ and $\hat{\phi}^k\in H_p$ such that

$$\begin{cases} a_f(\hat{u}_f^k,v)+b_f(v,\hat{p}_f^k) & +\gamma_2\int_\Gamma(\hat{u}_f^k\cdot n)(v\cdot n)\\ & =\gamma_2\int_\Gamma\hat{\sigma}^k(v\cdot n) \quad \forall v\in H_f,\\ b_f(\hat{u}_f^k,q)=0 & \forall q\in Q_f, \end{cases}$$

and

$$a_p(\hat{\phi}^k,\psi)+\frac{1}{\gamma_2}\int_\Gamma g\hat{\phi}^k\psi=\int_\Gamma \hat{\sigma}^k\psi \quad \forall \psi\in H_p.$$

Step 3. Set on Γ

$$\begin{aligned}\mu^{k+1} &= \mu^k-\theta[n\cdot(T(\hat{u}_f^k,\hat{p}_f^k)\cdot n)+g\hat{\phi}^k]\\ &=\mu^k-\theta[\gamma_2(\hat{\sigma}^k-\hat{u}_f^k\cdot n)+g\hat{\phi}^k],\end{aligned}$$

where $\theta>0$ is a further acceleration parameter.

It should be noted that Step 2 performs like a correction step for Step 1 in each iteration. Our new algorithm is developed based on Algorithm 0 and will be introduced in next subsection.

3.2. New algorithm construction

The new parallel DD algorithm is stated as follows.

Algorithm 1. Let $\eta_p^1=\eta_f^1=0$ be two assigned trace functions on Γ, and $\beta>0$ be the parameter which will be determined later based on ν and k_p for uniform convergence; then repeat the following two steps for $k=1,2,\ldots$ until convergence.

Step 1. Solve $(u_f^k,p_f^k)\in H_f\times Q_f$ and $\phi^k\in H_p$ such that

$$\begin{cases} a_f(u_f^k,v)+b_f(v,p_f^k) & +\beta\int_\Gamma(u_f^k\cdot n)(v\cdot n)\\ & =\int_\Gamma \eta_f^k(v\cdot n)+\int_{\Omega_f} f\cdot v \quad \forall v\in H_f,\\ b_f(u_f^k,q)=0 & \forall q\in Q_f,\end{cases} \tag{6}$$

and

$$\beta a_p(\phi^k,\psi)+\int_\Gamma g\phi^k\psi=\int_\Gamma \eta_p^k\psi \quad \forall\psi\in H_p. \tag{7}$$

This corresponds to imposing the following interface conditions for the Stokes and Darcy equations on Γ:

$$\begin{cases} n\cdot(T(u_f^k,p_f^k)\cdot n)+\beta u_f^k\cdot n &= \eta_f^k,\\ -\beta(k_p\nabla\phi^k)\cdot n+g\phi^k &= \eta_p^k.\end{cases} \tag{8}$$

Step 2. Set on Γ

$$\begin{cases} \eta_p^{k+1} &= 2\beta u_f^k\cdot n-\eta_f^k,\\ \eta_f^{k+1} &= \eta_p^k-2g\phi^k.\end{cases} \tag{9}$$

Remark 1. As a parallel Robin–Robin DD method, Algorithm 1 is similar to Algorithm 0. Their distinction lies as follows: (1) Algorithm 1 utilized two interface functions η_f and η_p for data exchange versus only one in Algorithm 0; (2) For each iteration, Algorithm 1 needs to solve Stokes and Darcy equations only once while Algorithm 0 needs twice. Therefore, Algorithm 1 only requires half of the iterative variables and arrays as in Algorithm 0 and thus has a simpler programming structure and needs less memory usage; (3) Algorithm 1 provides a specific error bound independent of ν and k_p as will be shown in Theorem 13, while Algorithm 0 has no such error estimate, even for its improved Aitken acceleration method. Comparison of numerical performance between these two algorithms conducted in Section 5 will show that Algorithm 1 outperforms Algorithm 0 when either ν or k_p tends to be small.

Let us show that Algorithm 1 is a good approximation of the coupling problem in the sense that once $\{u_f^k,p_f^k,\phi^k\}$ converge as $k\to\infty$, they will converge to the original analytic solution $\{u_f,p_f,\phi\}$.

Lemma 1. *Assume $\{u_f^k,p_f^k,\phi^k\}$ converge. Then they will converge to $\{u_f,p_f,\phi\}$.*

Proof. Suppose $\{u_f^k,p_f^k\}\to\{\hat{u},\hat{p}\}$ in $H_f\times Q_f$ and $\{\phi^k\}\to\hat{\phi}$ in H_p, respectively. Then taking the limits of (6) and (7) when $k\to\infty$ yields

$$\begin{cases} a_f(\hat{u},v)+b_f(v,\hat{p}) & +\beta\int_\Gamma(\hat{u}\cdot n)(v\cdot n)\\ & =\int_\Gamma \hat{\eta}_f(v\cdot n)+\int_{\Omega_f} f\cdot v \quad \forall v\in H_f,\\ b_f(\hat{u},q)=0 & \forall q\in Q_f,\end{cases} \tag{10}$$

and

$$\beta a_p(\hat{\phi},\psi)+\int_\Gamma g\hat{\phi}\psi=\int_\Gamma \hat{\eta}_p\psi \quad \forall\psi\in H_p, \tag{11}$$

where by taking the limits of (8),

$$\left\{\begin{array}{lcl} \hat{\eta}_f=\lim\limits_{k\to\infty}\eta_f^k &=& n\cdot(T(\hat{u},\hat{p})\cdot n)+\beta\hat{u}\cdot n\\ \hat{\eta}_p=\lim\limits_{k\to\infty}\eta_p^k &=& -\beta(k_p\nabla\hat{\phi})\cdot n+g\hat{\phi}\end{array}\right. \quad \text{on } \Gamma. \tag{12}$$

By putting the expressions of $\hat{\eta}_f$ and $\hat{\eta}_p$ in (12) into (10) and (11), respectively, we obtain

$$\begin{cases} a_f(\hat{u},v)+b_f(v,\hat{p}) & =\int_\Gamma n\cdot(T(\hat{u},\hat{p})\cdot n)+\int_{\Omega_f} f\cdot v \quad \forall v\in H_f,\\ b_f(\hat{u},q)=0 & \forall q\in Q_f,\end{cases}$$

and

$$a_p(\hat{\phi},\psi)=\int_\Gamma -(k_p\nabla\hat{\phi})\cdot n\psi \quad \forall\psi\in H_p.$$

Integration by parts immediately implies that $\{\hat{u},\hat{p}\}$ and $\hat{\phi}$ solve (1) and (2), respectively. Meanwhile, taking the limits of two equations in (9) yields

$$\begin{cases} \hat{\eta}_p &= 2\beta\hat{u}\cdot n-\hat{\eta}_f\\ \hat{\eta}_f &= \hat{\eta}_p-2g\hat{\phi}.\end{cases} \tag{13}$$

By putting (12) into (13) and noticing that $\beta>0$, we can show that

$$n\cdot(T(\hat{u},\hat{p})\cdot n)+g\hat{\phi}=(k_p\nabla\hat{\phi})\cdot n+\hat{u}\cdot n=0 \quad \text{on } \Gamma.$$

Therefore, $\{\hat{u},\hat{p}\}$ and $\{\hat{\phi}\}$ satisfy the interface condition (3). Meanwhile, $\hat{u}\in H_f$ satisfies (4) automatically from the definition of H_f. We conclude that $\{u_f^k,p_f^k,\phi^k\}$ will converge to the original analytic solution if they are convergent. In other words, Algorithm 1 is a well defined iterative method to solve the original coupling problem (1)–(4). □

3.3. Associated operators

In the following, we will show that the iterative solutions $\{u_f^k,p_f^k,\phi^k\}$ converge to the analytic solution $\{u_f,p_f,\phi\}$ where the convergence rates are insensitive to ν and k_p. To this end, let us introduce two Steklov–Poincaré operators T_p and T_f from $\Lambda=H_{00}^{\frac{1}{2}}(\Gamma)$ to its dual space Λ'.

Firstly, we define $T_p:\Lambda\to\Lambda'$ as follows: given $\chi\in\Lambda$,

$$T_p\chi=-\frac{k_p}{g}\frac{\partial R_p\chi}{\partial n},$$

where $R_p\chi\in H_p$ satisfies

$$\begin{cases} a_p(R_p\chi,\psi)=0 & \forall\psi\in H_0^1(\Omega_p)\\ R_p\chi=\chi & \text{on } \Gamma.\end{cases} \tag{14}$$

Then T_p satisfies the following weak formulation:

$$\langle T_p\chi,\mu\rangle=\frac{1}{g}a_p(R_p\chi,R_p\mu) \quad \forall\mu\in\Lambda. \tag{15}$$

Since $H_{00}^{\frac{1}{2}}(\Gamma)$ will be used frequently in the rest of our paper, let us review its definition (Chapter 1, [9]) here. At first, the Hilbert space $H^{\frac{1}{2}}(\Gamma)$ is assigned with the norm

$$\|\psi\|_{H^{\frac{1}{2}}(\Gamma)} = \left(\|\psi\|^2_{L^2(\Gamma)} + \int_\Gamma\int_\Gamma \frac{(\psi(x)-\psi(y))^2}{|x-y|^d}d\gamma d\gamma\right)^{\frac{1}{2}},$$

where $d = 2, 3$ is the dimension of the domain Ω and $d\gamma$ stands for the line or surface integral along Γ.

In order to define the subspace $H^{\frac{1}{2}}_{00}(\Gamma)$ of $H^{\frac{1}{2}}(\Gamma)$, let us introduce the distance function $d(x)$ to the boundary $\partial\Gamma$ of Γ:

$$d(x) = \mathrm{dist}(x, \partial\Gamma), \quad \forall x \in \Gamma.$$

The space $H^{\frac{1}{2}}_{00}(\Gamma)$ is then endowed with the norm

$$\|\psi\|_{H^{\frac{1}{2}}_{00}(\Gamma)} = \left(\|\psi\|^2_{H^{\frac{1}{2}}(\Gamma)} + \int_\Gamma \frac{\psi(x)^2}{d(x)}d\gamma\right)^{\frac{1}{2}}. \tag{16}$$

Secondly, We define $T_f : \Lambda \to \Lambda'$ in a similar way. Given $\chi \in \Lambda$,

$$T_f(\chi) = n \cdot (T(R^1_f\chi, R^2_f\chi) \cdot n),$$

where $(R^1_f\chi, R^2_f\chi) \in H_f \times Q_f$ satisfies

$$\begin{cases} a_f(R^1_f\chi, v) + b_f(v, R^2_f\chi) = 0 & \forall v \in (H^1_0(\Omega_f))^d \\ b_f(R^1_f\chi, q) = 0 & \forall q \in Q_f \\ R^1_f\chi \cdot n = \chi & \text{on} \quad \Gamma. \end{cases} \tag{17}$$

Then T_f satisfies the following weak formulation:

$$\langle T_f\chi, \mu\rangle = a_f(R^1_f\chi, R_1\mu) + b_f(R_1\mu, R^2_f\chi) \quad \forall \mu \in \Lambda, \tag{18}$$

where R_1 is any possible continuous extension from Λ to H_f such that $(R_1\mu) \cdot n = \mu$ on Γ.

T_p and T_f are both continuous and coercive as follows.

Lemma 2 (Lemma 2, Section 4.1 of [4]). *$T_f : \Lambda \to \Lambda'$ is a linear continuous and coercive operator satisfying*

$$|\langle T_f\chi, \mu\rangle| \leqslant C_f\nu\|\chi\|_\Lambda\|\mu\|_\Lambda,$$
$$\langle T_f\chi, \chi\rangle \geqslant c_f\nu\|\chi\|^2_\Lambda,$$

where $C_f \geqslant 1 \geqslant c_f > 0$ are generic constants depending on the measure of Ω_f.

Lemma 3. *$T_p : \Lambda \to \Lambda'$ is a linear continuous and coercive operator satisfying*

$$|\langle T_p\chi, \mu\rangle| \leqslant C_pk_p\|\chi\|_\Lambda\|\mu\|_\Lambda,$$
$$\langle T_p\chi, \chi\rangle \geqslant c_pk_p\|\chi\|^2_\Lambda,$$

where $C_p \geqslant 1 \geqslant c_p > 0$ are generic constants depending on the measure of Ω_p.

Proof. Eq. (14) implies that $R_p\chi$ can be regarded as a harmonic extension of χ, then there exists a positive constant $C_1 > 0$ independent of k_p [14] such that

$$\|R_p\chi\|_{H^1(\Omega_p)} \leqslant C_1\|\chi\|_\Lambda.$$

This inequality together with Cauchy–Schwarz inequality yields

$$\begin{aligned} |\langle T_p\chi, \mu\rangle| &= \frac{1}{g}a_p(R_p\chi, R_p\mu) \\ &\leqslant \frac{k_p}{g}\|R_p\chi\|_{H^1(\Omega_p)}\|R_p\mu\|_{H^1(\Omega_p)} \\ &\leqslant \frac{k_p}{g}(C_1)^2\|\chi\|_\Lambda\|\mu\|_\Lambda \\ &\leqslant C_pk_p\|\chi\|_\Lambda\|\mu\|_\Lambda, \end{aligned}$$

where $C_p = \max\left(\frac{C_1^2}{g}, 1\right) \geqslant 1$. Meanwhile, by noticing $R_p\chi = 0$ on Γ_p, we can apply Poincaré inequality [2] and the Trace theorem [14] to obtain

$$\begin{aligned} \langle T_p\chi, \chi\rangle &= \frac{1}{g}a_p(R_p\chi, R_p\chi) \\ &= \frac{k_p}{g}|R_p\chi|^2_{H^1(\Omega_p)} \\ &\geqslant \frac{k_p}{g}(C_2\|R_p\chi\|_{H^1(\Omega_p)})^2 \\ &\geqslant \frac{k_p}{g}(C_2C_3\|\chi\|_\Lambda)^2 \\ &\geqslant c_pk_p\|\chi\|^2_\Lambda, \end{aligned}$$

where $c_p = \min(\frac{C_2^2C_3^2}{g}, 1) \leqslant 1$. □

3.4. Error estimates

Let us set up the error estimates based on the operators T_p and T_f. Firstly, define the error terms $e^k_\phi = \phi^k - \phi$ in Ω_p, $e^k_u = u^k_f - u_f$ and $e^k_p = p^k_f - p_f$ in Ω_f, and $\tilde{\eta}^k_p = \eta^k_p - [-\beta k_p\frac{\partial\phi}{\partial n} + g\phi]$ and $\tilde{\eta}^k_f = \eta^k_f - [n \cdot (T(u_f, p_f) \cdot n) + \beta u_f \cdot n]$ on Γ. Since $\{u_f, p_f\}$ and ϕ satisfy Stokes Eq. (1) and Darcy Eq. (2), respectively, we apply integration by parts to (1) and (2) and obtain

$$\begin{cases} a_f(u_f, v) + b_f(v, p_f) + \beta\int_\Gamma(u_f \cdot n)(v \cdot n)ds \\ \quad = \int_\Gamma[n \cdot (T(u_f, p_f) \cdot n) + \beta u_f \cdot n](v \cdot n)ds + \int_{\Omega_f} f \cdot v dx \quad \forall v \in H_f, \\ b_f(u_f, q) = 0 \quad \forall q \in Q_f, \end{cases} \tag{19}$$

$$\beta a_p(\phi, \psi) + \int_\Gamma g\phi\psi ds = \int_\Gamma\left(-\beta k_p\frac{\partial\phi}{\partial n} + g\phi\right)\psi ds \quad \forall\psi \in H_p. \tag{20}$$

By subtracting (19) from (6) and (20) from (7), respectively, we obtain the following lemma.

Lemma 4. *Those error terms satisfy the following equations:*

$$\begin{cases} a_f(e^k_u, v) + b_f(v, e^k_p) & +\beta\int_\Gamma(e^k_u \cdot n)(v \cdot n)ds \\ & = \int_\Gamma\tilde{\eta}^k_f(v \cdot n)ds \quad \forall v \in H_f, \\ b_f(e^k_u, q) = 0 & \qquad \forall q \in Q_f, \end{cases} \tag{21}$$

and

$$\beta a_p(e^k_\phi, \psi) + \int_\Gamma ge^k_\phi\psi ds = \int_\Gamma\tilde{\eta}^k_p\psi ds \quad \forall\psi \in H_p. \tag{22}$$

In fact, with the help of the operators T_p and T_f, (21) and (22) can be interpreted as follows:

$$T_fe^k_u \cdot n + \beta e^k_u \cdot n = \tilde{\eta}^k_f,$$
$$\beta T_pge^k_\phi + ge^k_\phi = \tilde{\eta}^k_p,$$

which implies $e^k_u \cdot n$ and e^k_ϕ can be expressed as follows.

Lemma 5

$$e^k_u \cdot n = (T_f + \beta I)^{-1}\tilde{\eta}^k_f \quad \text{in } \Lambda \tag{23}$$

$$ge^k_\phi = (\beta T_p + I)^{-1}\tilde{\eta}^k_p \quad \text{in } \Lambda, \tag{24}$$

where $I : \Lambda \to \Lambda'$ is defined by using Riesz representation theorem: Given $\eta \in \Lambda$, $I\eta \in \Lambda'$ such that

$$(I\eta, \xi)_{\Lambda'} = \langle\xi, \eta\rangle \quad \forall\xi \in \Lambda',$$

with $(\cdot,\cdot)_{\Lambda'}$ denoting the inner product of Λ'. Then $\|I\eta\|_{\Lambda'} = \|\eta\|_\Lambda$.

Meanwhile, the definition of $\tilde{\eta}^k_f$, the formula of η^k_f in Algorithm 1, and the interface condition (3) yield

$$\begin{aligned}\tilde{\eta}_f^{k+1} =&\eta_f^{k+1} - [n\cdot(T(u_f,p_f)\cdot n) + \beta u_f\cdot n]\\ =&[\eta_p^k - 2g\phi^k] - \left[-g\phi - \beta k_p\frac{\partial\phi}{\partial n}\right]\\ =&\left(\eta_p^k - \left[-\beta k_p\frac{\partial\phi}{\partial n} + g\phi\right]\right) - 2(g\phi^k - g\phi)\\ =&\tilde{\eta}_p^k - 2ge_\phi^k. \end{aligned}\tag{25}$$

Similarly, we obtain

$$\tilde{\eta}_p^{k+1} = 2\beta e_u^k\cdot n - \tilde{\eta}_f^k.\tag{26}$$

Putting (24) into (25) and (23) into (26) yields

$$\begin{aligned}\tilde{\eta}_f^{k+1} =&\tilde{\eta}_p^k - 2(\beta T_p + I)^{-1}\tilde{\eta}_p^k\\ =&[(\beta T_p + I) - 2I](\beta T_p + I)^{-1}\tilde{\eta}_p^k\\ =&(\beta T_p - I)(\beta T_p + I)^{-1}\tilde{\eta}_p^k,\end{aligned}$$

and

$$\begin{aligned}\tilde{\eta}_p^{k+1} =&2\beta(T_f + \beta I)^{-1}\tilde{\eta}_f^k - \tilde{\eta}_f^k\\ =&[2\beta I - (T_f + \beta I)](T_f + \beta I)^{-1}\tilde{\eta}_f^k\\ =&(\beta I - T_f)(\beta I + T_f)^{-1}\tilde{\eta}_f^k.\end{aligned}$$

Then $\tilde{\eta}_p^k$ and $\tilde{\eta}_f^k$ have the following iterative relations.

Lemma 6. *If we define two operators in Λ', $S_p = (\beta T_p - I)(\beta T_p + I)^{-1}$ and $S_f = (\beta I - T_f)(\beta I + T_f)^{-1}$, then*

$$\begin{cases}\tilde{\eta}_f^{k+1} &= S_p\tilde{\eta}_p^k &= S_pS_f\tilde{\eta}_f^{k-1}\\ \tilde{\eta}_p^{k+1} &= S_f\tilde{\eta}_f^k &= S_fS_p\tilde{\eta}_p^{k-1}.\end{cases}$$

Therefore, if we can show that S_fS_p and S_pS_f are contractive operators in Λ' such that $\|S_f\|\cdot\|S_p\| \leqslant \rho < 1$ uniformly for any values of ν and k_p, we can conclude that $\|\tilde{\eta}_f^k\|_{\Lambda'}$ and $\|\tilde{\eta}_p^k\|_{\Lambda'}$ converge to zero with the convergence rates independent of both ν and k_p.

Theorem 7. *The operators $S_f, S_p : \Lambda' \to \Lambda'$ satisfy*

$$\|S_p\| \leqslant \sqrt{\frac{1 - 2\beta\cdot c_pk_p + \beta^2\cdot C_p^2k_p^2}{1 + 2\beta\cdot c_pk_p + \beta^2\cdot C_p^2k_p^2}} < 1,$$

$$\|S_f\| \leqslant \sqrt{\frac{\beta^2 - 2\beta\cdot c_f\nu + C_f^2\nu^2}{\beta^2 + 2\beta\cdot c_f\nu + C_f^2\nu^2}} < 1.$$

Proof

$$\frac{\|S_p\mu\|_{\Lambda'}^2}{\|\mu\|_{\Lambda'}^2} = \frac{\|(\beta T_p - I)(\beta T_p + I)^{-1}\mu\|_{\Lambda'}^2}{\|\mu\|_{\Lambda'}^2}.$$

Let $\eta = (\beta T_p + I)^{-1}\mu \in \Lambda$, then $\mu = (\beta T_p + I)\eta$ and we have

$$\begin{aligned}\frac{\|S_p\mu\|_{\Lambda'}^2}{\|\mu\|_{\Lambda'}^2} =&\frac{\|(\beta T_p - I)\eta\|_{\Lambda'}^2}{\|(\beta T_p + I)\eta\|_{\Lambda'}^2}\\ =&\frac{\beta^2\|T_p\eta\|_{\Lambda'}^2 - 2\beta(T_p\eta, I\eta) + \|I\eta\|_{\Lambda'}^2}{\beta^2\|T_p\eta\|_{\Lambda'}^2 + 2\beta(T_p\eta, I\eta) + \|I\eta\|_{\Lambda'}^2}\\ =&\frac{\beta^2\|T_p\eta\|_{\Lambda'}^2 - 2\beta\langle T_p\eta, \eta\rangle + \|\eta\|_{\Lambda}^2}{\beta^2\|T_p\eta\|_{\Lambda'}^2 + 2\beta\langle T_p\eta, \eta\rangle + \|\eta\|_{\Lambda}^2}\\ \leqslant&\frac{\beta^2\|T_p\eta\|_{\Lambda'}^2 - 2\beta\cdot c_pk_p\|\eta\|_{\Lambda}^2 + \|\eta\|_{\Lambda}^2}{\beta^2\|T_p\eta\|_{\Lambda'}^2 + 2\beta\cdot c_pk_p\|\eta\|_{\Lambda}^2 + \|\eta\|_{\Lambda}^2}\\ =&\frac{1 - 2\beta\cdot c_pk_p + \beta^2\cdot\frac{\|T_p\eta\|_{\Lambda'}^2}{\|\eta\|_{\Lambda}^2}}{1 + 2\beta\cdot c_pk_p + \beta^2\cdot\frac{\|T_p\eta\|_{\Lambda'}^2}{\|\eta\|_{\Lambda}^2}}\\ \leqslant&\frac{1 - 2\beta\cdot c_pk_p + \beta^2\cdot C_p^2k_p^2}{1 + 2\beta\cdot c_pk_p + \beta^2\cdot C_p^2k_p^2},\end{aligned}$$

where the first inequality holds since T_p is coercive by Lemma 3 and $f(x) = \frac{a-bx}{a+bx}$ is a decreasing function with $f' > 0$ when $a, b > 0$, while the last inequality holds due to the continuity of T_p in Lemma 3 and the fact that $f(x) = \frac{a+cx}{b+cx}$ is an increasing function with $f' > 0$ when $b > a$ and $c > 0$.

Therefore,

$$\|S_p\| = \sup_{\mu\in\Lambda'}\frac{\|S_p\mu\|_{\Lambda'}}{\|\mu\|_{\Lambda'}} \leqslant \sqrt{\frac{1 - 2\beta\cdot c_pk_p + \beta^2\cdot C_p^2k_p^2}{1 + 2\beta\cdot c_pk_p + \beta^2\cdot C_p^2k_p^2}} < 1.$$

$\|S_f\|$ can be estimated similarly. □

Remark 2. Theorem 7 implies that Algorithm 1 is always convergent when $\beta > 0$. However, the upper bounds of $\|S_p\|$, $\|S_f\|$ and thus $\|S_p\|\cdot\|S_f\|$ may tend to one if both k_p and ν tend to zero. Therefore, the convergence rates of $\tilde{\eta}_p^k$ and $\tilde{\eta}_f^k$ are deteriorated and the required number of iterations can become very large when k_p and ν are small. In order to make sure at least one norm is uniformly bounded below $\rho < 1$, which is enough to ensure $\|S_p\|\cdot\|S_f\| \leqslant \rho < 1$ by Theorem 7, we need to determine β adaptively as shown in the following three theorems which consider all possible scenarios of k_p and ν. Since both k_p and ν cannot tend to infinity under any circumstances, it is reasonable to assume $k_p, \nu < M$ for a fixed value $M > 0$ from now on.

Theorem 8. *Suppose $1 \leqslant k_p < M$ and $1 \leqslant \nu_p < M$ are well above zero. If we set $\beta = 1$, then $\|S_p\|$, $\|S_f\|$ and $\|S_p\|\cdot\|S_f\|$ are uniformly bounded by a constant less than one for all such k_p and ν,*

$$\|S_p\| \leqslant \sqrt{\frac{1 - 2c_pM + C_p^2M^2}{1 + 2c_pM + C_p^2M^2}} < 1,$$

$$\|S_f\| \leqslant \sqrt{\frac{1 - 2c_fM + C_f^2M^2}{1 + 2c_fM + C_f^2M^2}} < 1,$$

$$\|S_p\|\cdot\|S_f\| \leqslant \sqrt{\frac{1 - 2c_pM + C_p^2M^2}{1 + 2c_pM + C_p^2M^2}}\cdot\sqrt{\frac{1 - 2c_fM + C_f^2M^2}{1 + 2c_fM + C_f^2M^2}} < 1.$$

Proof. From Theorem 7 with $\beta = 1$, we have

$$\|S_p\| \leqslant \sqrt{\frac{1 - 2c_pk_p + C_p^2k_p^2}{1 + 2c_pk_p + C_p^2k_p^2}}.$$

By defining an auxiliary function $f(x) = \frac{1-2c_px+C_p^2x^2}{1+2c_px+C_p^2x^2}$ and noticing $C_p \geqslant 1 \geqslant c_p > 0$, we get $f'(x) = \frac{4c_p(C_p^2x^2-1)}{(1+2c_px+C_p^2x^2)^2} > 0$ wherever $x \geqslant 1$. Therefore, $f(x)$ is an increasing function so that

$$\|S_p\| \leqslant \sqrt{f(k_p)} < \sqrt{f(M)} = \sqrt{\frac{1 - 2c_pM + C_p^2M^2}{1 + 2c_pM + C_p^2M^2}} < 1.$$

Estimate of $\|S_f\|$ can be set up similarly. Combination of $\|S_p\|$ and $\|S_f\|$ concludes the proof. □

Therefore, we can simply set the parameter $\beta = 1$ to ensure uniform convergence of Algorithm 1 when both k_p and ν do not tend to zero. Next, let us consider the scenarios when either k_p or ν becomes small.

Theorem 9. *Suppose $0 < k_p < 1$. If we set $\beta = \frac{1}{M_pk_p}$ where $M_p > 1$ is an arbitrarily fixed constant, then $\|S_f\|$ and $\|S_p\|\cdot\|S_f\|$ are uniformly bounded by a constant less than one for all such k_p and any values of $\nu > 0$.*

$$\|S_p\| \leqslant \sqrt{\frac{M_p^2 - 2c_pM_p + C_p^2}{M_p^2 + 2c_pM_p + C_p^2}} < 1,$$

$$\|S_p\| \cdot \|S_f\| \leqslant \sqrt{\frac{M_p^2 - 2c_pM_p + C_p^2}{M_p^2 + 2c_pM_p + C_p^2}} < 1.$$

Furthermore, when we set $M_p = C_p$, the above norm bound attains its minimum value $\sqrt{\frac{C_p - c_p}{C_p + c_p}}$ to ensure the best convergence rate.

Proof. Theorem 7 provides an upper bound of $\|S_p\|$ as follows:

$$\|S_p\| \leqslant \sqrt{\frac{1 - 2\beta c_pk_p + \beta^2C_p^2k_p^2}{1 + 2\beta c_pk_p + \beta^2C_p^2k_p^2}}.$$

It is obvious that choosing $\beta = \frac{1}{M_pk_p}$ for a fixed constant $M_p > 1$ will eliminate k_p in the above expression to obtain

$$\|S_p\| \leqslant \sqrt{\frac{M_p^2 - 2c_pM_p + C_p^2}{M_p^2 + 2c_pM_p + C_p^2}} < 1.$$

Meanwhile, $\|S_f\| < 1$ always holds from Theorem 7. Therefore,

$$\|S_p\| \cdot \|S_f\| \leqslant \sqrt{\frac{M_p^2 - 2c_pM_p + C_p^2}{M_p^2 + 2c_pM_p + C_p^2}} < 1.$$

In order to find the optimal M_p to achieve the minimal upper bound for $\|S_p\| \cdot \|S_f\|$, let us consider the function of M_p inside the square root:

$$f(M_p) = \frac{M_p^2 - 2c_pM_p + C_p^2}{M_p^2 + 2c_pM_p + C_p^2}.$$

Direct computation yields

$$f'(M_p) = \frac{4c_p(M_p + C_p)(M_p - C_p)}{(M_p^2 + 2c_pM_p + C_p^2)^2}.$$

It is obvious that $M_p = C_p$ is the only critical point of $f(M_p)$ which achieves its minimum value there. Therefore, if we set $\beta = \frac{1}{C_pk_p}$ in Algorithm 1, we get

$$\|S_p\| \cdot \|S_f\| \leqslant \sqrt{f(C_p)} = \sqrt{\frac{C_p - c_p}{C_p + c_p}} < 1. \quad \square$$

Remark 3. Although Algorithm 1 converges for any value of $M_p > 1$, the best convergence rate is achieved when $M_p = C_p$. However, C_p depends on the measure of Ω_p and cannot be determined exactly. Numerical tests from Section 5 have verified that Algorithm 1 is not quite sensitive to the parameter $\beta = \frac{1}{M_pk_p}$ so that the optimal value of M_p can be chosen from a wide range. The following Algorithm MP is proposed in order to find an ideal value of M_p which is a good approximation to C_p.

Let us define a function $\zeta \in \Lambda = H_{00}^{\frac{1}{2}}(\Gamma)$ which equals to 1 almost everywhere in the interior of Γ and drops down to zero continuously near $\partial\Gamma$ in order to satisfy zero boundary condition. To simplify the description, let us restrict to 2D case while 3D case can be handled similarly. Assume Γ is expressed by a piecewise smooth bijective function $h : [0, 1] \to \Gamma$ where $h(0)$ and $h(1)$ denote the endpoints of Γ. Then $\zeta(x)$ is defined as follows:

$$\zeta(x) = \begin{cases} \frac{h^{-1}(x)}{0.01} & x \in h([0, 0.01)) \\ 1 & x \in h([0.01, 0.99]) \\ \frac{1 - h^{-1}(x)}{0.01} & x \in h((0.99, 1]), \end{cases} \tag{27}$$

By setting $k_p = 1$ and $\chi = \mu = \zeta$ in Lemma 3, we obtain

$$|\langle T_p\zeta, \zeta\rangle| = \frac{1}{g} a_p(R_p\zeta, R_p\zeta) \leqslant C_p \cdot \|\zeta\|_\Lambda^2.$$

Therefore, $M_p = \frac{a_p(R_p\zeta, R_p\zeta)}{g \cdot \|\zeta\|_\Lambda^2} \leqslant C_p$ is considered as a good approximation to C_p where $\|\zeta\|_\Lambda$ is calculated from the half-norm definition (16).

Algorithm MP. Compute $M_p = \frac{a_p(\phi, \phi)}{g \cdot \|\zeta\|_\Lambda^2}$ where $k_p = 1$ and $\phi \in H_p$ satisfies

$$\begin{cases} a_p(\phi, \psi) = 0 & \forall \psi \in H_0^1(\Omega_p), \\ \phi = \zeta & \text{on } \Gamma. \end{cases} \tag{28}$$

Theorems 8 and 9 are concerned with two scenarios of either small $k_p < 1$ with arbitrary ν or large $k_p \geqslant 1$ with large $\nu \geqslant 1$. The remaining scenario of large $k_p \geqslant 1$ with small $\nu < 1$ is considered in the following theorem, whose proof is similar to that of Theorem 9.

Theorem 10. *Suppose $0 < \nu < 1$ and $1 \leqslant k_p < M$. If we set $\beta = M_f\nu$ where $M_f > 1$ is an arbitrarily fixed constant, then $\|S_f\|$ and $\|S_p\| \cdot \|S_f\|$ are uniformly bounded by a constant less than one for all such ν and k_p.*

$$\|S_f\| \leqslant \sqrt{\frac{M_f^2 - 2c_fM_f + C_f^2}{M_f^2 + 2c_fM_f + C_f^2}} < 1,$$

$$\|S_p\| \cdot \|S_f\| \leqslant \sqrt{\frac{M_f^2 - 2c_fM_f + C_f^2}{M_f^2 + 2c_fM_f + C_f^2}} < 1.$$

Furthermore, when we set $M_f = C_f$, the above norm bound attains its minimum value $\sqrt{\frac{C_f - c_f}{C_f + c_f}}$ to ensure the best convergence rate.

Proof. Theorem 7 provides an upper bound of $\|S_f\|$ as follows:

$$\|S_f\| \leqslant \sqrt{\frac{\beta^2 - 2\beta \cdot c_f\nu + C_f^2\nu^2}{\beta^2 + 2\beta \cdot c_f\nu + C_f^2\nu^2}} < 1.$$

It is obvious that choosing $\beta = M_f\nu$ for a fixed constant $M_f > 1$ will eliminate ν in the above expression to obtain

$$\|S_f\| \leqslant \sqrt{\frac{M_f^2 - 2c_fM_f + C_f^2}{M_f^2 + 2c_fM_f + C_f^2}} < 1.$$

Meanwhile, $\|S_p\| < 1$ always holds from Theorem 7. Therefore,

$$\|S_p\| \cdot \|S_f\| \leqslant \sqrt{\frac{M_f^2 - 2c_fM_f + C_f^2}{M_f^2 + 2c_fM_f + C_f^2}} < 1.$$

In order to find the optimal M_f to achieve the minimal upper bound for $\|S_p\| \cdot \|S_f\|$, let us consider the function of M_f inside the square root:

$$f(M_f) = \frac{M_f^2 - 2c_fM_f + C_f^2}{M_f^2 + 2c_fM_f + C_f^2}.$$

Direct computation yields

$$f'(M_f) = \frac{4c_f(M_f + C_f)(M_f - C_f)}{(M_f^2 + 2c_fM_f + C_f^2)^2}.$$

It is obvious that $M_f = C_f$ is the only critical point of $f(M_f)$ which achieves its minimum value there. Therefore, if we set $\beta = C_f\nu$ in Algorithm 1, we get

$$\|S_p\| \cdot \|S_f\| \leqslant \sqrt{\frac{C_f - c_f}{C_f + c_f}} < 1. \quad \square$$

Remark 4. Similarly as in Remark 3, it is impossible to determine the optimal value $M_f = C_f$ which depends on the measure of Ω_f. The following Algorithm MF is then proposed in order to find an ideal value of $M_f > 1$ which is a good approximation to C_f. To this end, we set $v = 1$ and $\chi = \mu = \zeta$ in Lemma 2 to obtain

$$|\langle T_f \zeta, \zeta \rangle| = a_f(R_f^1 \zeta, R_f^1 \zeta) \leqslant C_f \cdot \|\zeta\|_{\Lambda}^2.$$

Therefore, $M_f = \frac{a_f(R_f^1\zeta, R_f^1\zeta)}{\|\zeta\|_\Lambda^2} \leqslant C_f$ performs as a good approximation to C_f.

Algorithm MF. Compute $M_f = \frac{a_f(u,u)}{\|\zeta\|_\Lambda^2}$ where $v = 1$ and $(u, p) \in H_f \times Q_f$ satisfies

$$\begin{cases} a_f(u, v) + b_f(v, p) = 0 & \forall v \in (H_0^1(\Omega_f))^d \\ b_f(u, q) = 0 & \forall q \in Q_f \\ u \cdot n = \zeta & \text{on} \quad \Gamma \end{cases} \tag{29}$$

where the tangential components of u equal to zero on Γ automatically due to the definition of H_f.

Combination of Theorems 8–10 and Lemma 6 yields the following convergence theorem.

Theorem 11. *Suppose the parameter β be chosen adaptively as follows: $\beta = 1$ when $k_p \geqslant 1$ and $v \geqslant 1$; $\beta = \frac{1}{M_p k_p}$ with an ideal value of $M_p > 1$ determined from Algorithm MP when $0 < k_p < 1$ and v is arbitrary; $\beta = M_f v$ with an ideal value of $M_f > 1$ determined from Algorithm MF when $0 < v < 1$ and $k_p \geqslant 1$. The error term sequences $\{\tilde{\eta}_p^k\}_{k=1}^{\infty}$ and $\{\tilde{\eta}_f^k\}_{k=1}^{\infty}$ converge to zero with the convergence rate ρ independent of both k_p and v,*

$$\|\tilde{\eta}_p^k\|_{\Lambda'} \leqslant C\rho^k, \quad \|\tilde{\eta}_f^k\|_{\Lambda'} \leqslant C\rho^k,$$

where C is a generic domain dependent constant, $M > 0$ is the upper bound of both v and k_p, and

$$\rho = \max \left(\sqrt{\frac{1-2c_pM+C_p^2M^2}{1+2c_pM+C_p^2M^2}} \cdot \sqrt{\frac{1-2c_fM+C_f^2M^2}{1+2c_fM+C_f^2M^2}}, \right. \\ \left. \sqrt{\frac{M_p^2-2c_pM_p+C_p^2}{M_p^2+2c_pM_p+C_p^2}}, \quad \sqrt{\frac{M_f^2-2c_fM_f+C_f^2}{M_f^2+2c_fM_f+C_f^2}} \right) < 1.$$

Finally, let us apply Lemmas 4 and 5 to show that $\{e_u^k, e_p^k, e_\phi^k\}$ share the same convergence property.

Theorem 12. *The error sequences $\{e_u^k, e_p^k, e_\phi^k\}$ satisfy for a generic constant C which depends on the measure of Ω_p and Ω_f,*

$$\|e_u^k\|_{H^1(\Omega_f)} \leqslant C\|\tilde{\eta}_f^k\|_{\Lambda'}, \quad \|e_p^k\|_{L^2(\Omega_f)} \leqslant C\|\tilde{\eta}_f^k\|_{\Lambda'}, \quad \|e_\phi^k\|_{H^1(\Omega_p)} \leqslant C\|\tilde{\eta}_p^k\|_{\Lambda'}.$$

Proof. From the second equation in Lemma 5, we have

$$\begin{aligned} \|e_\phi^k\|_\Lambda &\leqslant \frac{1}{g}\|(\beta T_p + I)^{-1}\| \cdot \|\tilde{\eta}_p^k\|_{\Lambda'} \\ &= \frac{1}{g} \sup_{\mu \in \Lambda'} \frac{\|(\beta T_p + I)^{-1}\mu\|_\Lambda}{\|\mu\|_{\Lambda'}} \cdot \|\tilde{\eta}_p^k\|_{\Lambda'}. \end{aligned}$$

Let $\eta = (\beta T_p + I)^{-1}\mu \in \Lambda$, then $\mu = (\beta T_p + I)\eta$ and we have

$$\begin{aligned} \frac{\|(\beta T_p + I)^{-1}\mu\|_\Lambda^2}{\|\mu\|_{\Lambda'}^2} &= \frac{\|\eta\|_\Lambda^2}{\|(\beta T_p + I)\eta\|_{\Lambda'}^2} \\ &= \frac{\|\eta\|_\Lambda^2}{\beta^2\|T_p\eta\|_{\Lambda'}^2 + 2\beta\langle T_p\eta, \eta\rangle + \|I\eta\|_{\Lambda'}^2} \\ &\leqslant \frac{\|\eta\|_\Lambda^2}{\|I\eta\|_{\Lambda'}^2} = \frac{\|\eta\|_\Lambda^2}{\|\eta\|_\Lambda^2} = 1, \end{aligned}$$

Therefore,

$$\|e_\phi^k\|_\Lambda \leqslant \frac{1}{g}\|\tilde{\eta}_p^k\|_{\Lambda'}.$$

Furthermore, since $e_\phi^k = \phi^k - \phi$ in Ω_p can be regarded as a harmonic extension of e_ϕ^k on Γ, then

$$\|e_\phi^k\|_{H^1(\Omega_p)} \leqslant C_1\|e_\phi^k\|_\Lambda \leqslant \frac{C_1}{g}\|\tilde{\eta}_p^k\|_{\Lambda'}. \tag{30}$$

Similarly, we can show that

$$\|e_u^k\|_{H^1(\Omega_f)} \leqslant C_2\|\tilde{\eta}_f^k\|_{\Lambda'}. \tag{31}$$

Finally, let us estimate $\|e_p^k\|_{L^2(\Omega_p)}$. Since $e_p^k \in L^2(\Omega_f)$, there exists $w \in (H_0^1(\Omega_f))^d$, $w \neq 0$ such that

$$\alpha_0\|e_p^k\|_{L^2(\Omega_f)}\|w\|_{H^1(\Omega_f)} \leqslant -b_f(w, e_p^k),$$

where $\alpha_0 > 0$ is the inf–sup condition satisfied by $b_f(v, p)$, and the H^1-norm of the vector function $w = (w_1, \ldots, w_d)$ is defined as

$$\|w\|_{H^1(\Omega_f)}^2 = \sum_{k=1}^{d}\|w_k\|_{H^1(\Omega_f)}^2.$$

Replacing v by w in (21) of Lemma 4 and noticing that $w = 0$ on Γ, we have

$$\|e_p^k\|_{L^2(\Omega_f)}\|w\|_{H^1(\Omega_f)} \leqslant \frac{1}{\alpha_0}a_f(e_u^k, w) \leqslant \frac{C_3}{\alpha_0}\|e_u^k\|_{H^1(\Omega_f)}\|w\|_{H^1(\Omega_f)}.$$

Therefore,

$$\|e_p^k\|_{L^2(\Omega_f)} \leqslant \frac{C_3}{\alpha_0}\|e_u^k\|_{H^1(\Omega_f)} \leqslant \frac{C_3C_2}{\alpha_0}\|\tilde{\eta}_f^k\|_{\Lambda'}. \tag{32}$$

Taking $C = \max(\frac{C_1}{g}, C_2, \frac{C_3C_2}{\alpha_0})$ finishes the proof. □

Theorems 12 and 11 yield the main result of this paper as follows.

Theorem 13. *If the parameters β is set adaptively as in Theorem 11, the iterative solutions $\{u_f^k, p_f^k, \phi^k\}$ in Algorithm 1 converge to the original analytic solution $\{u_f, p_f, \phi\}$ where the convergence rates are independent of k_p and v,*

$$\|u_f^k - u_f\|_{H^1(\Omega_f)} \leqslant C\rho^k, \quad \|p_f^k - p_f\|_{L^2(\Omega_f)} \leqslant C\rho^k, \quad \|\phi^k - \phi\|_{H^1(\Omega_p)} \leqslant C\rho^k,$$

where $C > 0$ is a domain dependent constant and $0 < \rho < 1$ is specified in Theorem 11.

4. Finite element discretization

On the domain $\Omega = \Omega_p \bigcup \Omega_f$, we set up a regular triangulations Σ_h of size $h > 0$ made up of triangles if $d = 2$ or tetrahedra if $d = 3$ such that the sub-triangulations Σ_{ph} in Ω_p and Σ_{fh} in Ω_f are compatible on Γ, i.e., they have the same partition $\Sigma_{\gamma h}$ on Γ.

We apply Taylor–Hood mixed finite element on Σ_{fh} and P_2 finite element on Σ_{ph} to approximate the original coupling problem (1)–(4). Some conforming finite element spaces are defined to approximate H_f, Q_f, H_p and Λ,

$$\begin{aligned} H_{fh} &= \{v \in (V_{fh})^d : v \cdot \tau_j|_\Gamma = 0, \quad 1 \leqslant j \leqslant d-1\}, \\ Q_{fh} &= \{q_h \in C(\Omega_f) : q_h|_T \in P_1(T) \quad \forall T \in \Sigma_{fh}\}, \\ H_{ph} &= \{\psi_h \in C(\Omega_p) : \psi_h|_T \in P_2(T) \quad \forall T \in \Sigma_{ph}, \psi_h = 0 \text{ on } \Gamma_p\}, \\ \Lambda_h &= \{\eta_h \in L^2(\Gamma) : \eta_h|_\tau \in P_2(\tau) \quad \forall \tau \in \Sigma_{\gamma h}\}, \end{aligned}$$

where

$$V_{fh} = \{v_h \in C(\Omega_f) : v_h|_T \in P_2(T) \forall T \in \Sigma_{fh}, v_h = 0 \text{ on } \Gamma_f\}.$$

Then we have that $v_h \cdot n \in \Lambda_h$ for any $v_h \in H_{fh}$ and $\psi_h|_\Gamma \in \Lambda_h$ for any $\psi_h \in H_{ph}$. Since conforming finite elements are utilized here, we have $H_{fh} \subset H_f$, $Q_{fh} \subset Q_f$, $H_{ph} \subset H_p$ and $\Lambda_h \subset \Lambda$.

The analytic problem (1)–(4) is then discretized as follows.

Find $(u_{fh}, p_{fh}) \in H_{fh} \times Q_{fh}$, $\phi_h \in H_{ph}$ such that

$$\left\{\begin{array}{lcl} a_f(u_{fh}, v_h) & + & b_f(v_h, p_{fh}) + g a_p(\phi_h, \psi_h) + \int_\Gamma g\phi_h(v_h \cdot n) \\ & & -\int_\Gamma g\psi_h(u_{fh} \cdot n) \\ & = & \int_{\Omega_f} f \cdot v_h \quad \forall v_h \in H_{fh}, \quad \psi_h \in H_{ph}, \\ b_f(u_{fh}, q_h) & = & 0 \quad \forall q_h \in Q_{fh}. \end{array}\right. \tag{33}$$

The discretized DD method to solve the finite element problem (33) becomes:

Let $\eta^1_{ph} = \eta^1_{fh} = 0$ be two assigned trace functions in Λ_h, and $\beta > 0$ be the parameter determined based on v and k_p as in Theorem 11. Then repeat the following steps for $k = 1, 2, \ldots$ until convergence.

Step 1. Find $(u^k_{fh}, p^k_{fh}) \in H_{fh} \times Q_{fh}$ and $\phi^k_h \in H_{ph}$ such that

$$\left\{\begin{array}{ll} a_f(u^k_{fh}, v_h) + b_f(v_h, p^k_{fh}) & +\beta \int_\Gamma (u^k_{fh} \cdot n)(v_h \cdot n) \\ & = \int_\Gamma \eta^k_{fh}(v_h \cdot n) + \int_{\Omega_f} f \cdot v_h \quad \forall v_h \in H_{fh}, \\ b_f(u^k_{fh}, q_h) = 0 & \forall q_h \in Q_{fh}, \end{array}\right. \tag{34}$$

and

$$\beta a_p(\phi^k_h, \psi_h) + \int_\Gamma g\phi^k_h \psi_h = \int_\Gamma \eta^k_{ph}\psi_h \quad \forall \psi_h \in H_{ph}. \tag{35}$$

Step 2. Set on Γ

$$\left\{\begin{array}{ll} \eta^{k+1}_{ph} & = 2\beta u^k_{fh} \cdot n - \eta^k_{fh}, \\ \eta^{k+1}_{fh} & = \eta^k_{ph} - 2g\phi^k_h. \end{array}\right. \tag{36}$$

Since the discretized problem has the same formulation as the original analytic problem, we can simply follow the procedures of Section 3 to show the uniform convergence of $\{u^k_{fh}, p^k_{fh}, \phi^k_h\}$ towards $\{u_{fh}, p_{fh}, \phi_h\}$. To this end, let us introduce the discretized Steklov–Poincaré operators $T_{ph}, T_{fh} : \Lambda_h \to \Lambda'_h$ as follows.

For any $\chi_h \in \Lambda_h$, $T_{ph}\chi_h$ satisfies

$$\langle T_{ph}\chi_h, \mu_h\rangle = \frac{1}{g} a_p(R_{ph}\chi_h, R_{ph}\mu_h) \quad \forall \mu_h \in \Lambda_h, \tag{37}$$

where $R_{ph}\chi_h \in H_{ph}$ is the solution to

$$\left\{\begin{array}{ll} a_p(R_{ph}\chi_h, \psi_h) = 0 & \forall \psi_h \in H^0_{ph} = \{v \in H_{ph} | v = 0 \text{ on } \Gamma\}, \\ R_{ph}\chi_h = \chi_h & \text{on } \Gamma. \end{array}\right. \tag{38}$$

For any $\chi_h \in \Lambda_h$, $T_{fh}\chi_h$ satisfies

$$\langle T_{fh}\chi_h, \mu_h\rangle = a_f(R^1_{fh}\chi_h, R_{1h}\mu_h) + b_f(R_{1h}\mu_h, R^2_{fh}\chi_h) \quad \forall \mu_h \in \Lambda_h, \tag{39}$$

where R_{1h} is any possible continuous extension from Λ_h to H_{fh} such that $(R_{1h}\mu_h) \cdot n = \mu_h$ on Γ for all $\mu_h \in \Lambda_h$, and $(R^1_{fh}\chi_h, R^2_{fh}\chi_h) \in H_{fh} \times Q_{fh}$ is the solution to

$$\left\{\begin{array}{ll} a_f(R^1_{fh}\chi_h, v_h) + b_f(v_h, R^2_{fh}\chi_h) = 0 & \forall v_h \in H^0_{fh}, \\ b_f(R^1_{fh}\chi_h, q_h) = 0 & \forall q_h \in Q_{fh}, \\ R^1_{fh}\chi_h \cdot n = \chi_h & \text{on} \quad \Gamma, \end{array}\right. \tag{40}$$

where $H^0_{fh} = \{v \in H_{fh} : v \cdot n|_\Gamma = 0\}$. The above discrete operators T_{ph} and T_{fh} have the following properties.

Lemma 14 (Lemma 1, Section 4.1 of [5]). *$T_{fh} : \Lambda_h \to \Lambda'_h$ is a linear continuous and coercive operator satisfying*

$$|\langle T_{fh}\chi_h, \mu_h\rangle| \leqslant \tilde{C}_f v \|\chi_h\|_\Lambda \|\mu_h\|_\Lambda,$$
$$\langle T_{fh}\chi_h, \chi_h\rangle \geqslant \tilde{c}_f v \|\chi_h\|^2_\Lambda,$$

where $\tilde{C}_f \geqslant 1 \geqslant \tilde{c}_f > 0$ are generic constants independent of both v and h.

Lemma 15. *$T_{ph} : \Lambda_h \to \Lambda'_h$ is a linear continuous and coercive operator satisfying*

$$|\langle T_{ph}\chi_h, \mu_h\rangle| \leqslant \tilde{C}_p k_p \|\chi_h\|_\Lambda \|\mu_h\|_\Lambda$$
$$\langle T_{ph}\chi_h, \chi_h\rangle \geqslant \tilde{c}_p k_p \|\chi_h\|^2_\Lambda,$$

where $\tilde{C}_p \geqslant 1 \geqslant \tilde{c}_p > 0$ are generic constants independent of both k_p and h.

Proof. By replacing ψ_h by $R_{ph}\chi_h - H_h\chi_h$ in equation (38), where H_h is the Galerkin approximation of the harmonic extension operator defined in (44) of [4], we have

$$a_p(R_{ph}\chi_h, R_{ph}\chi_h) = a_p(R_{ph}\chi_h, H_h\chi_h).$$

The Uniform Extension Theorem (Theorem 4.1.3, [16]) says that there exists a positive constant $\tilde{\alpha} > 0$ depending on the measure of Ω_p, but independent of h, such that

$$\|H_h\chi_h\|_{H^1(\Omega_p)} \leqslant \tilde{\alpha}\|\chi_h\|_\Lambda, \quad \forall \chi_h \in \Lambda_h.$$

Therefore,

$$\begin{aligned} |R_{ph}\chi_h|^2_{H^1(\Omega_p)} &= \frac{1}{k_p} a_p(R_{ph}\chi_h, R_{ph}\chi_h) \\ &= \frac{1}{k_p} a_p(R_{ph}\chi_h, H_h\chi_h) \\ &\leqslant \frac{1}{k_p} k_p |R_{ph}\chi_h|_{H^1(\Omega_p)} \cdot |H_h\chi_h|_{H^1(\Omega_p)} \\ &\leqslant |R_{ph}\chi_h|_{H^1(\Omega_p)} \cdot \tilde{\alpha}\|\chi_h\|_\Lambda, \end{aligned}$$

i.e.,

$$|R_{ph}\chi_h|_{H^1(\Omega_p)} \leqslant \tilde{\alpha}\|\chi_h\|_\Lambda.$$

This inequality together with Cauchy–Schwarz inequality yields

$$\begin{aligned} |\langle T_{ph}\chi_h, \mu_h\rangle| &= \frac{1}{g} a_p(R_{ph}\chi_h, R_{ph}\mu_h) \\ &\leqslant \frac{k_p}{g} |R_{ph}\chi_h|_{H^1(\Omega_p)} \cdot |R_{ph}\mu_h|_{H^1(\Omega_p)} \\ &\leqslant \frac{k_p}{g} \tilde{\alpha}^2 \|\chi_h\|_\Lambda \cdot \|\mu_h\|_\Lambda \\ &\leqslant \tilde{C}_p k_p \|\chi\|_{\Lambda_h} \|\mu_h\|_\Lambda, \end{aligned}$$

where $\tilde{C}_p = \max(\frac{\tilde{\alpha}^2}{g}, 1)$. Meanwhile, application of Poincaré inequality and the Trace theorem yields

$$\begin{aligned} \langle T_{ph}\chi_h, \chi_h\rangle &= \frac{1}{g} a_p(R_{ph}\chi_h, R_{ph}\chi_h) \\ &= \frac{k_p}{g} |R_{ph}\chi_h|^2_{H^1(\Omega_p)} \\ &\geqslant \frac{k_p}{g} (C_1 \|R_{ph}\chi_h\|_{H^1(\Omega_p)})^2 \\ &\geqslant \frac{k_p}{g} (C_1 C_2 \|\chi_h\|_\Lambda)^2 \\ &\geqslant \tilde{c}_p k_p \|\chi_h\|^2_\Lambda, \end{aligned}$$

where $\tilde{c}_p = \min\left(\frac{C_1^2 C_2^2}{g}, 1\right)$. □

Lemmas 14 and 15 show that T_{ph} and T_{fh} are still as continuous and coercive as their analytic counterparts while the constants $\tilde{C}_p$, $\tilde{c}_p$ and $\tilde{C}_f$, $\tilde{c}_f$ are independent of k_p, v as well as the mesh size h. We can simply follow along the direction of Section 3 to set up a similar uniform convergence result as follows.

Theorem 16. *Let the parameter β be set adaptively as follows: $\beta = 1$ when $k_p \geqslant 1$ and $v \geqslant 1$; $\beta = \frac{1}{\tilde{M}_p k_p}$ with an ideal $\tilde{M}_p$ value determined from the discretized version of Algorithm MP when $0 < k_p < 1$ and v is arbitrary; $\beta = \tilde{M}_f v$ with an ideal $\tilde{M}_f$ value determined from the discretized version of Algorithm MF when $0 < v < 1$ and $k_p \geqslant 1$. The iterative solutions $\{u^k_{fh}, p^k_{fh}, \phi^k_h\}$ defined in (34)–(36) converge to* *the finite element solution* $\{u_{fh}, p_{fh}, \phi_h\}$ *of (33) where the convergence rates are independent of* k_p, ν *and the mesh size* h.

$$\|u_{fh}^k - u_{fh}\|_{H^1(\Omega_f)} \leqslant \tilde{C}\tilde{\rho}^k, \quad \|p_{fh}^k - p_{fh}\|_{L^2(\Omega_f)} \leqslant \tilde{C}\tilde{\rho}^k,$$
$$\|\phi_h^k - \phi_h\|_{H^1(\Omega_p)} \leqslant \tilde{C}\tilde{\rho}^k,$$

where $\tilde{C} > 0$ *and* $0 < \tilde{\rho} < 1$ *are domain dependent constants with*

$$\tilde{\rho} = \max\left(\sqrt{\frac{1-2\tilde{c}_p M+\tilde{C}_p^2 M^2}{1+2\tilde{c}_p M+\tilde{C}_p^2 M^2}} \cdot \sqrt{\frac{1-2\tilde{c}_f M+\tilde{C}_f^2 M^2}{1+2\tilde{c}_f M+\tilde{C}_f^2 M^2}}, \sqrt{\frac{\tilde{M}_p^2-2\tilde{c}_p\tilde{M}_p+\tilde{C}_p^2}{\tilde{M}_p^2+2\tilde{c}_p\tilde{M}_p+\tilde{C}_p^2}}, \sqrt{\frac{\tilde{M}_f^2-2\tilde{c}_f\cdot\tilde{M}_f+\tilde{C}_f^2}{\tilde{M}_f^2+2\tilde{c}_f\cdot\tilde{M}_f+\tilde{C}_f^2}}\right) < 1.$$

5. Numerical example

We consider a domain $\Omega \subset R^2$ with $\Omega_f = (0,1)\times(1,2)$, $\Omega_p = (0,1)\times(0,1)$ and $\Gamma = (0,1)\times 1$. Boundary conditions and the right hand side f are chosen such that the exact solution of the coupled Stokes–Darcy problem is $u_f = (y^2 - 2y + 1, x^2 - x)$, $p_f = 2\nu(x + y - 1) + 1/(3k_p)$, $\phi = [(x(1-x)(y-1) + \frac{y^3}{3} - y^2 + y]/k_p + 2\nu x$, with ν and k_p constant in Ω_f and Ω_p, respectively. We assume $g = 1$.

We apply Taylor–Hood finite element to approximate the Stokes problem, and quadratic Lagrangian elements to approximate Darcy equation. A relative tolerance of $\epsilon = 10^{-4}$ is imposed for the error control so that the iteration will stop at step k when

$$\max\left(\frac{|u_{fh}^k - u_{fh}^{k-1}|}{|u_{fh}^k| + \epsilon_0}, \frac{|p_{fh}^k - p_{fh}^{k-1}|}{|p_{fh}^k| + \epsilon_0}, \frac{|\phi_h^k - \phi_h^{k-1}|}{|\phi_h^k| + \epsilon_0}\right) < \epsilon,$$

where $\epsilon_0 = 10^{-7}$ is used to avoid division by zero.

All the test programs are written by C++ and run on Dell Inspiron E520 Desktop with Intel Core(TM)2 Duo 1.86 GHz CPU and 1G RAM.

5.1. Parameter independence tests

Table 1 shows that the number of iterations are under control by simply setting $\beta = 1$ when $\nu \geqslant 1$ and $k_p \geqslant 1$. We can observe that the number of iteration is indeed independent of the mesh size h.

When $k_p < 1$ is small, we first apply the discretized version of Algorithm MP to obtain $M_p \approx 12.0$. Table 2 then shows that the number of iterations from Algorithm 1 is stable with arbitrary values of k_p when we set the parameter $\beta = \frac{1}{M_p k_p}$ adaptively.

As to the remaining situation where $\nu < 1$ and $k_p \geqslant 1$, we apply the discretized version of Algorithm MF to obtain $M_f \approx 50.0$. Table 3 also shows that the number of iterations is stable when we set $\beta = M_f \nu$ in Algorithm 1.

5.2. Algorithm comparison tests

In order to compare the numerical performance of Algorithm 0 by Discacciati et al. [6] and Algorithm 1 proposed here, we solve the above example by using both algorithms respectively with the same mesh size $h = \frac{1}{48}$ and the same tolerance. We then evaluate the total number of iteration steps for each algorithm. Since the working load of one iteration in Algorithm 0 is actually twice that of Algorithm 1, we double the number of iteration steps of Algorithm 0 for the fairness of comparison. Table 4 compares the iteration numbers for Algorithm 0 with optimal parameters γ_1, γ_2 and Algorithm 1.

The table shows that when $k_p \geqslant 1$ and $\nu \geqslant 1$, both algorithms achieve similar efficiencies while Algorithm 0 requires less iteration steps than Algorithm 1. However, when either k_p or ν tends to zero, Algorithm 1 still keeps the same efficiency while Algorithm 0 demonstrates a much poorer performance. Therefore, Algorithm 1 is stable with parameter variation while Algorithm 0 becomes deteriorated when the parameters ν or k_p tend to be small.

It should be noted that an Aitken acceleration technique is also applied to Algorithm 0 in [6] so that its numerical performance is greatly improved when ν and k_p are small. However, Algorithm 1 has a simpler structure and is also stable with inherent parameter variation without necessity of any acceleration technique, which prevents us from providing specific estimates on the error reduction factors in Theorems 13 and 16.

5.3. Sensitivity tests

To validate the sensitivity of Algorithm 1 to variation of parameter β, we consider three scenarios with different values of ν and k_p. Fig. 2 shows that under all circumstances, the total number of iterations is stable when β is chosen from a wide range close to its optimal value. Therefore, Algorithm 1 is not quite sensitive to β and provides us computational convenience in choosing β to solve coupled Stokes and Darcy flows.

5.4. Convergence rate tests

In order to verify the convergence rate of the iterative solution towards the given analytic solution $\{u_f, p_f, \phi\}$, the error sequences $\|u_{fh}^n - u_f\|_{H^1(\Omega_f)}$, $\|p_{fh}^n - p_f\|_{L^2\Omega_f}$ and $\|\phi_h^n - \phi\|_{H^1(\Omega_p)}$ are reported in

Table 1
Number of iterations when $\nu \geqslant 1$ and $k_p \geqslant 1$.

(ν, k_p)	β	$h_1 = \frac{1}{12}$	$h_2 = \frac{1}{24}$	$h_3 = \frac{1}{48}$
(1.0, 1.0)	1.0	28	32	33
(5.0, 5.0)	1.0	32	32	35
(10.0, 5.0)	1.0	29	32	35
(15.0, 20.0)	1.0	36	36	32

Table 2
Number of iterations when $k_p < 1$ and ν is arbitrary.

(ν, k_p)	β	$h_1 = \frac{1}{12}$	$h_2 = \frac{1}{24}$	$h_3 = \frac{1}{48}$
$(10.0, 10^{-2})$	8.33	49	54	60
$(1.0, 10^{-2})$	8.33	52	57	61
$(10^{-2}, 10^{-2})$	8.33	35	45	45
$(1.0, 10^{-3})$	83.3	33	35	39
$(1.0, 10^{-4})$	833	35	45	45

Table 3
Number of iterations when $\nu < 1$ and $k_p \geqslant 1$.

(ν, k_p)	β	$h_1 = \frac{1}{12}$	$h_2 = \frac{1}{24}$	$h_3 = \frac{1}{48}$
$(10^{-1}, 1.0)$	5.0	48	55	59
$(10^{-2}, 1.0)$	0.5	34	38	41
$(10^{-2}, 2.0)$	0.5	39	44	48
$(10^{-3}, 1.0)$	0.05	53	57	61

Table 4
Number of iterations for Algorithms 0 and 1 with different ν and k_p.

(ν, k_p)	Iterations for Algorithm 0(γ_1, γ_2)	Iterations for Algorithm 1 (β)
(5.0, 5.0)	10 (1.0, 1.0)	35 (1.0)
(1.0, 1.0)	14 (1.0, 1.0)	33 (1.0)
$(1.0, 10^{-3})$	248 (1.0, 1000)	39 (83.3)
$(10^{-2}, 10^{-2})$	410 (0.01, 100)	45 (8.33)
$(10^{-2}, 1.0)$	294 (0.01, 1.0)	41 (0.5)
$(10^{-3}, 1.0)$	296 (0.001, 1.0)	61 (0.05)

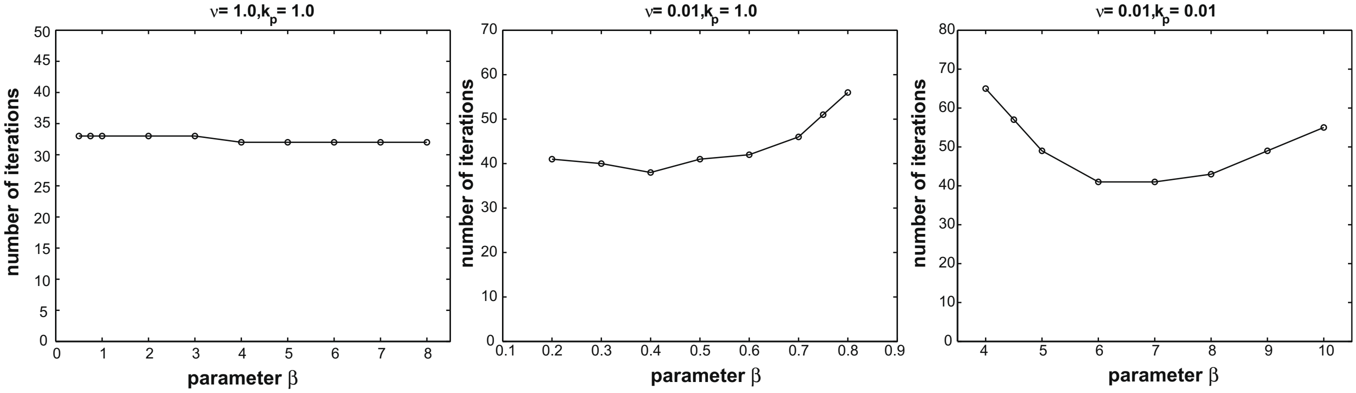

Fig. 2. Number of iterations versus parameter β.

Table 5 where the parameters are set to $k_p = \nu = 1.0$, $\beta = 1.0$ and $h = \frac{1}{48}$. Fig. 3 shows that the logarithms of the above error sequences seem like linear functions of iteration step n. This matches with the theoretical error estimates reported in Theorems 13 and 16.

The convergence plot also exhibits stagnation of all the iteration errors after iteration step 16. This is due to the fact that $\|u_{fh}^n - u_f\|_{H^1(\Omega_f)}$ is composed of an iterative error term $\|u_{fh}^n - u_{fh}\|_{H^1(\Omega_f)}$ which obeys Theorem 16 and a discretization error term $\|u_{fh} - u_f\|_{H^1(\Omega_f)}$ which only depends on h. When n is small, the discretization error term can be ignored compared with the dominating iterative error term whose logarithm is a linear function of n as observed; While n becomes large, the iterative error tends to be small so that stagnation happens due to the discretization error term which cannot be ignored. Same explanations also apply for $\|p_{fh}^n - p_f\|_{L^2\Omega_f}$ and $\|\phi_h^n - \phi\|_{H^1(\Omega_p)}$.

Table 5
Convergence of the iterative solutions towards the analytic solution.

n	$\|u_{fh}^n - u_f\|_{H^1(\Omega_f)}$	$\|p_{fh}^n - p_f\|_{L^2(\Omega_f)}$	$\|\phi_h^n - \phi\|_{H^1(\Omega_p)}$
1	1.19e−1	1.15e0	6.46e−1
6	9.63e−3	1.01e−1	6.53e−2
11	1.52e−3	8.49e−3	6.93e−3
16	3.48e−4	8.14e−4	7.86e−4
21	9.56e−5	1.13e−4	4.13e−4
26	7.82e−5	8.67e−5	4.08e−4
31	7.78e−5	8.52e−5	4.07e−4

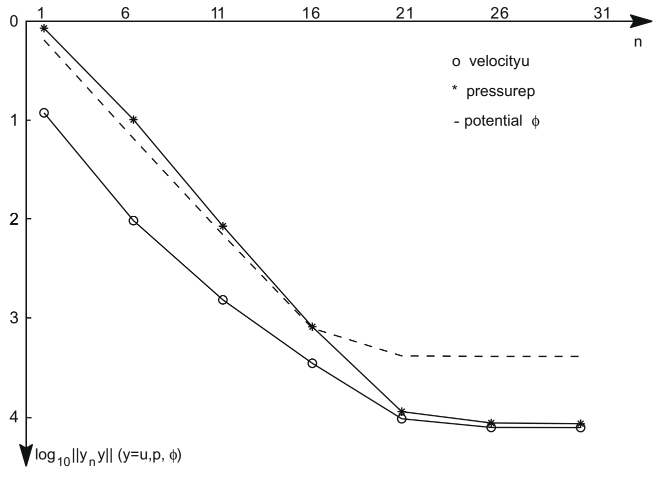

Fig. 3. Convergence of the iterative solutions.

6. Conclusion and future work

In this paper, we constructed a robust parallel algorithm to accurately model the coupling of surface and groundwater flows. The non-overlapping DD method is used to decouple the original problem in the fluid and porous media regions. Taylor–Hood mixed finite element method and P_2 finite element method are used to discretize the fluid and porous media problems, respectively. The error estimate of the iterative solution towards the original solution is provided to show convergence of the algorithm. Meanwhile, the algorithm is insensitive to the viscosity ν of the fluid and the hydraulic conductivity k_p of the porous medium by choosing the parameter β adaptively.

In the future, we will apply non-matching grids in the fluid and porous regions to fulfill different meshing requirement. This will provide great flexibility in constructing parallel algorithms to solve coupled fluid and porous media problems whose domains can be discretized independently.

References

[1] F. Brezzi, M. Fortin, Mixed and Hybrid Finite Element Methods, Springer-Verlag, New York, 1991.
[2] P.G. Ciarlet, The Finite Element Method for Elliptic Problems, North-Holland Publishing Company, Amsterdam, 1979.
[3] M. Discacciati, E. Miglio, A. Quarteroni, Mathematical and numerical models for coupling surface and groundwater flows, Appl. Num. Math. 43 (2002) 57–74.
[4] M. Discacciati, A. Quarteroni, Analysis of a domain decomposition method for the coupling of Stokes and Darcy equations, in: F. Brezzi et al. (Eds.), Numerical Mathematics and Advanced Applications. Proceedings of ENUMATH 2001, Springer, Milan, 2003, pp. 3–20.
[5] M. Discacciati, A. Quarteroni, Convergence analysis of a subdomain iterative method for the finite element approximation of the coupling of Stokes and Darcy equations, Comput. Visual. Sci. 6 (2004) 93–103.
[6] M. Discacciati, A. Quarteroni, A. Valli, Robin–Robin domain decomposition methods for the Stokes–Darcy coupling, SIAM J. Numer. Anal. 45 (2007) 1246–1268.
[7] J.C. Galvis, M. Sarkis, Balancing domain decomposition methods for mortar coupling Stokes–Darcy systems, in: Proceedings of the 16th International Conference on Domain Decomposition Methods, Springer-Verlag, 2006.
[8] D. Gartling, C. Hickox, R. Givler, Simulation of coupled viscous and porous flow problems, Compos. Fluid Dyn. 7 (1996) 23–48.
[9] P. Grisvard, Elliptic Problems in Nonsmooth Domains, Pitman Publisher, Boston, 1985.
[10] W. Jager, A. Mikelic, On the interface boundary condition of Beavers, Joseph and Saffman, SIAM J. Appl. Math. 60 (2000) 1111–1127.
[11] B. Jiang, J.C. Bruch Jr., J.M. Sloss, A nonoverlapping domain decomposition method for variational inequalities derived from free boundary problems, Numer. Methods Part. Diff. Eqn. 22 (2006) 1–17.
[12] B. Jiang, Convergence analysis of P1 finite element method for free boundary problems on nonoverlapping subdomains, Comput. Methods Appl. Mech. Engrg. 196 (2006) 371–378.
[13] W.L. Layton, F. Schieweck, I. Yotov, Coupling fluid flow with porous media flow, SIAM J. Numer. Anal. 40 (2003) 2195–2218.

[14] J.L. Lions, E. Magenes, Non-homogeneous Boundary Value Problems and Applications, vol. I, Springer-Verlag, New York, 1972.
[15] K.A. Mardal, X.C. Tai, R. Winther, A robust finite element method for Darcy–Stokes flow, SIAM J. Numer. Anal. 40 (2002) 1605–1631.
[16] A. Quarteroni, A. Valli, Domain Decomposition Method for Partial Differential Equations, Oxford University Press, Oxford, 1999.
[17] B. Riviere, I. Yotov, Locally conservative coupling of Stokes and Darcy flows, SIAM J. Numer. Anal. 42 (2005) 1959–1977.
[18] A. Salinger, R. Aris, I. Derby, Finite element formulations for large-scale, coupled flows in adjacent porous and open fluid domains, Int. J. Numer. Methods Fluids 18 (1994) 1185–1209.